Cerebral Cortex May 2011;21:1178–1191
doi:10.1093/cercor/bhq188
Advance Access publication October 18, 2010

Neural Correlates of Developing and Adapting Behavioral Biases in Speeded Choice Reactions—An fMRI Study on Predictive Motor Coding

Simon B. Eickhoff[1,2,3], Witali Pomjanski[4], Oliver Jakobs[4], Karl Zilles[2,3,4] and Robert Langner[1,2,3]

[1]Department of Psychiatry and Psychotherapy, RWTH Aachen University, 52074 Aachen, Germany, [2]Institute of Neuroscience and Medicine (INM-2), Research Centre Jülich, 52425 Jülich, Germany, [3]Jülich–Aachen Research Alliance (JARA-Brain) and [4]C. & O. Vogt Institute for Brain Research, University of Düsseldorf, 40225 Düsseldorf, Germany

Address correspondence to Dr Simon B. Eickhoff, Institut für Medizin (IME), Forschungszentrum Jülich GmbH, D-52425 Jülich, Germany. Email: s.eickhoff@fz-juelich.de.

In reaction-time (RT) tasks with unequally probable stimuli, people respond faster and more accurately in high-probability trials than in low-probability trials. We used functional magnetic resonance imaging to investigate brain activity during the acquisition and adaptation of such biases. Participants responded to arrows pointing to either side with different and previously unknown probabilities across blocks, which were covertly reversed in the middle of some blocks. Changes in response bias were modeled using the development of the selective RT bias at the beginning of a block and after the reversal as parametric regressors. Both fresh development and reversal of an existing response bias were associated with bilateral activations in inferior parietal lobule, intraparietal sulcus, and supplementary motor cortex. Further activations were observed in right temporoparietal junction, dorsolateral prefrontal cortex, and dorsal premotor cortex. Only during initial development of biases at the beginning of a block, we observed additional activity in ventral premotor cortex and anterior insula, whereas the basal ganglia (bilaterally) were recruited when the bias was adapted to reversed probabilities. Taken together, these areas constitute a network that updates and applies implicit predictions to create an attention and motor bias according to environmental probabilities that transform into specific facilitation.

Keywords: functional imaging, implicit prediction, preparation, probability learning, response bias

Introduction

Studies on speeded 2-choice reactions, with 2 responses mapped onto 2 stimuli, consistently find that unequal stimulus frequencies lead to faster (and more correct) responses to the more likely stimulus—a finding referred to as the "probability effect" (Laming 1969; Blackman 1972; Heuer 1982; Miller 1998; Lungu et al. 2004). The size of this effect is reported to be about 60–70 ms for a 75–80% preponderance of one of the stimuli (Laming 1969; Miller 1998; Lungu et al. 2004). This suggests that the brain represents and uses this probability information to predict, selectively prepare, and facilitate movements (Miller 1998).

Understanding how the brain uses the probability context of events to facilitate corresponding action will greatly benefit from examining how time-related changes in event predictability are learned and represented. In contrast to previous efforts (e.g., Strange et al. 2005; Bestmann et al. 2008), we did not examine associations of brain activity with theoretically derived, a priori measures of predictability but instead derived predictors from actual response behavior. In our view, such empirical measures reflect subjective representations of situational probabilities more validly. Furthermore, our predictors did not reflect trial-by-trial levels of static measures of predictability but rather represented the trial-wise amount of change thereof (see below).

Recently, Kilner et al. (2007) proposed that predictive motor coding underlies the generation and adjustment of movements, describing how predictions are implemented in motor cognition. They postulated several hierarchical levels of action preparation that form a forward system of information processing from a general intention to the movement of individual muscles. Complementary to this intention-driven (top-down) system of motor control, a corresponding bottom-up system processes sensory (feedback) information and interacts with it to form a hierarchical Bayesian system. Thus, motor responses may be selectively sped up by top-down-driven (and bottom-up-confirmed) biases toward the more frequent and, hence, predicted movement (Miller 1998). This does not exclude prediction benefits at perceptual levels, since contextual, for example, visual, information may also be differentially anticipated within the overarching intention (see, e.g., Schultz and Lennert 2009, on attentional bias shifts toward more frequent target dimensions).

An important component of hierarchical predictive coding is the presence of prediction errors that provide feedback to higher hierarchical levels and can hence drive an adaptation of predictions and behavior (Friston 2002; Fletcher and Frith 2009). While higher-level regions compute a probabilistic model of future sensory input and the hereby required motor commands, lower levels evaluate predicted against actual input (Kilner et al. 2007; Friston and Kiebel 2009) and generate a prediction error reflecting the difference between both. A low error indicates a valid prediction whose associated movement components should be reinforced. A high prediction error, on the other hand, indicates that the internal model may not provide an appropriate representation of the current environment (Friston 2002; Courville et al. 2006; Friston et al. 2006; Kilner et al. 2007; Jakobs et al. 2009). Thus, in order to minimize future prediction errors and facilitate faster processing, the previous sensorimotor model is updated by incorporating current sensory data (Behrens et al. 2007). For a graphical summary of the model, see Figure 1.

Exploiting the behavioral consequences of unequal stimulus–response probabilities, we aimed to delineate brain areas subserving the probability effect. We used a blocked 2-choice reaction-time (RT) task with stimuli indicating a left or right response, respectively, occurring in 20% versus 80% of the trials. Additionally, in half the blocks, we implemented

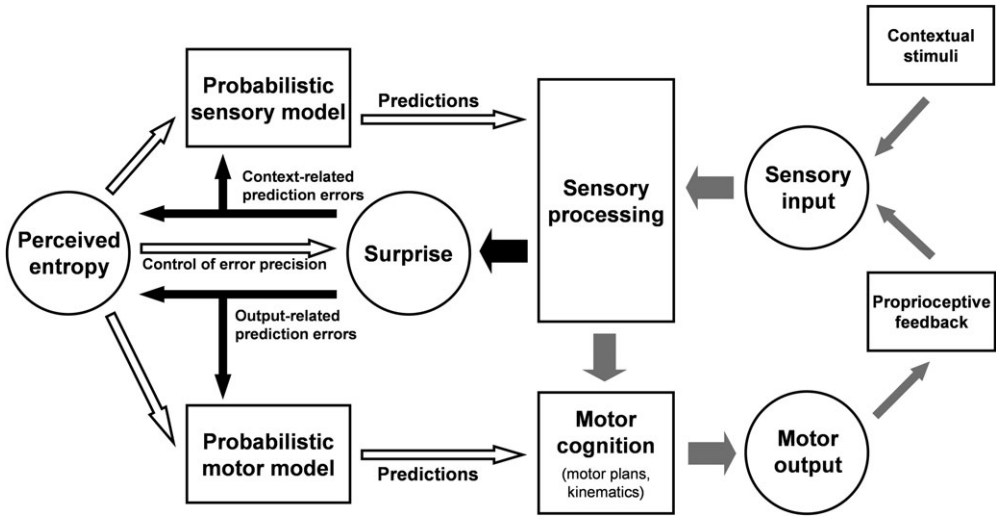

Figure 1. A summary of the theoretical framework of predictive coding in the motor domain. Predictions are conveyed via cortical feedback loops and lead to selective facilitative adjustments at various levels of the lower sensorimotor hierarchy, here collectively labeled "sensory processing" and "motor cognition." Surprise reflects the deviation of sensory input (produced by motor output or situational context) from these predictions; weighted by their precision, the resulting prediction errors are transmitted via feedforward connections to higher cortical levels, where they lead to evaluations and—if necessary—adjustments of probability models and perceived entropy (i.e., predictability). See text for details.

a probability reversal after about half the trials, as there should be substantial overlap but also differences in the neural correlates of initial bias development and bias adaptation.

As the blocks begin equally often with a preponderance of left or right cues, respectively, participants should start off into each block with "flat" priors, that is, unbiased predictions (but see Behrens et al. 2007, for the concept of overarching volatility priors). The development of a response bias toward the more frequent stimulus then implies that stimulus probability distributions are integrated over trials, increasingly shaping predictions about upcoming events. In information-theoretic terms (cf. Strange et al. 2005), the maximal entropy (i.e., averaged uncertainty) at the outset of each block should diminish over time, whereas the difference between surprise intensities associated with either response cue should grow. According to the predictive-coding framework outlined above, this information then facilitates the processing of the more likely outcome and produces the behavioral bias (Miller 1998). As long as the probabilities remain unchanged, the predictions appear valid and are therefore sustained. Hence, during the start of each block, the initially flat priors become skewed to reflect the current environment increasingly correctly until most stimuli (i.e., the frequent ones) contain little surprise, that is, new information.

In cases of a probability reversal, the starting situation is different: biased predictions are already established, since task-relevant probability information has been gathered and integrated during previous trials. Thus, entropy is rather small. Now that probabilities are reversed, the current predictions become invalid, and the previous behavioral advantage of their application turns into a disadvantage. In other words, a large prediction error is now elicited during most trials (i.e., the previous low-probability alternative), leading to an adjustment of predictions at higher levels. Specifically, amassing prediction errors should be initially encountered by giving more weight to bottom-up sensory information, reflecting a subjective increase in entropy (which objectively remains constant after the reversal). After reaching a maximum, perceived entropy returns to lower levels over time, whereas initially large differences between surprise at occurrence of either alternative first vanish and then, in reversed form, reappear, reflecting the readjusted bias. The main difference between the 2 situations (i.e., initial vs. postreversal bias establishment) therefore is the different baseline situation. At the beginning of a block, due to flat priors (i.e., great entropy), there should be no surprise (i.e., no prediction error) at either outcome. In contrast, at probability reversal it should mainly be prediction errors, amassing during low entropy, that signal a change in environment and drive the adjustment of internal models.

Both processes, however, can be regarded as aspects of predictive motor coding. Thus, core areas of a network subserving predictive motor coding should not only be active for the acquisition and modulation of biased models but their recruitment should accord with the dynamics of the behavioral change that derives from these models. Here, we investigated their neural basis by functional magnetic resonance imaging (fMRI). We expected predictive-coding–related activity in frontal regions such as the supplementary motor area (SMA), lateral pre-motor cortex (PMC), and the dorsolateral prefrontal cortex (DLPFC), that is, regions associated with response selection (Casey et al. 2001; Wang et al. 2009), visuomotor mapping (Passingham et al. 2000; Jakobs et al. 2009), and monitoring of movement execution (Nachev et al. 2008). Moreover, given the role of the inferior parietal lobule (IPL) and intraparietal sulcus (IPS) in spatial attention and stimulus–response mapping (Vandenberghe and Gillebert 2009) and of the cerebellum in different aspects of prediction processing (Wolpert and Kawato 1998; Blakemore and Sirigu 2003; Pollok et al. 2008), these structures may also contribute to predictive motor coding.

Materials and Methods

Participants

We examined 20 healthy volunteers (age range 21–47, mean age 28.7 years; 7 females) without any record of neurological or psychiatric

disorders and normal or corrected-to-normal vision. All subjects gave written informed consent to the study protocol, which had been approved by the local ethics committee of the RWTH Aachen University Hospital. Participants were right-handed, as determined by the Edinburgh Handedness Inventory (Oldfield 1971).

Task and Stimuli

The task was to react as fast and correctly as possible to arrows pointing to either the left or right side, which were presented briefly (200 ms) with a size of 4° viewing angle in the central field of view. Responses were given by pressing a button on an MRI-compatible response pad (LumiTouch) with the corresponding index finger. All visual stimuli were presented using the Presentation software package (Version 11.0, Neurobehavioral Systems Inc.) and displayed on a custom-built, shielded TFT screen (14° × 8° viewing angle) at the rear end of the scanner, visible via a mirror mounted on the head coil. Before the start of the experiment, participants were familiarized with the task by instruction and a short practice session outside the scanner.

We used a design in which task periods were periodically alternated with resting baseline periods of 20-s duration each. Each task period started with the instruction "Achtung" ("attention"), indicating that the next one was about to start. The instruction was displayed on the screen for 500 ms and was followed by a blank interval (empty screen), whose duration was uniformly jittered between 1200 and 1400 ms. Then, the arrows were presented for 200 ms each. The interval between subsequent arrows was uniformly jittered between 600 and 800 ms to prevent the temporal anticipation of the stimuli (cf. Jakobs et al. 2009) as well as to optimize the variance in the blood oxygen level–dependent (BOLD) signal time series. Likewise, in order to prevent anticipation of the next baseline period potentially inducing a decrease in alertness toward the end of a block, the total number of events per block was varied between 24 and 30 in the following fashion: Each task period was divided into 2 parts, each containing 12–15 stimuli (uniformly jittered). Both parts followed each other immediately, such that participants did not notice a change. Thus, the total length of each task block varied between 21.6 and 27.0 s (mean: 24.3 s).

Experimental Conditions

The first aim of this study was to investigate the neural correlates of the development of a response bias, that is, the integration of previous experience into predictions as well as the increasing application of these. The second aim was to delineate the neural substrates of adapting predictions to changing task demands, that is, the dynamic modification of these predictions when they do not match anymore with the current stimulus–response probabilities. These aims were pursued by employing the following experimental setup.

Constant Probability—No-Change Condition

Here, the percentage of arrows pointing to either the left or right side remained constant throughout the entire block, that is, across the first and second part. In half the no-change condition (NCC) blocks, 80% of the arrows pointed to the left and 20% to the right. In the other half, this ratio was inverted. Importantly, participants were not told that the probabilities would be biased a priori, so that they would have to learn the dominance of a given side purely based on the history of trials in the current block.

Variable Probability—Change Condition

The first part of a block from this condition, that is, the first 12–15 events, equaled the first part of a NCC block. In the second part of these blocks, however, stimulus–response probabilities were covertly reversed. That is, if a block started out with 80% probability for leftward-pointing arrows, there would be a switch to 80% probability for rightward-pointing arrows in the second part. This was the case in half the change condition (CC) blocks. The other half started out with 80% of the arrows pointing to the right and switched to 80% of them pointing to the left in the second part.

Across the whole experiment, we presented 20 NCC blocks and 30 CC blocks. Block order was pseudorandomized so that participants could not predict the nature of the upcoming condition and the initial probability distribution. Accordingly, the participants' expectations should have been unbiased (flat) at the start of each block and could only develop based on the history of the events within that block. The transition between the 2 parts (i.e., the change in probability) was not indicated in any explicit way. The first event of the second part followed the last one of the first part within the usual stimulus onset asynchrony (SOA) range, and the position of the transition was jittered (occurring after 12–15 trials).

fMRI

Images were acquired on a Siemens Trio 3-T whole-body scanner using BOLD contrast (gradient-echo echo-planar imaging [EPI] pulse sequence, repetition time = 1.6 s, echo time = 30 ms, flip angle = 90°, in-plane resolution = 3.1 × 3.1 mm, 36 axial slices [3.1-mm thickness] covering the entire brain). Image acquisition was preceded by 4 dummy images allowing for magnetic field saturation. These were discharged prior to further processing. Images were analyzed using SPM5 (www.fil.ion.ucl.ac.uk/spm).

First, the EPI images were corrected for head movement by affine registration using a 2-pass procedure, by which images were initially realigned to the first image and subsequently to the mean of the realigned images. After realignment, the mean EPI image for each subject was spatially normalized to the Montreal Neurological Institute (MNI) single subject template (Holmes et al. 1998) using the "unified segmentation" approach (Ashburner and Friston 2003). The resulting parameters of a discrete cosine transform, which define the deformation field necessary to move the subjects data into the space of the MNI tissue probability maps, were then combined with the deformation field transforming between the latter and the MNI single subject template. The ensuing deformation was subsequently applied to the individual EPI volumes that were hereby transformed into the MNI single subject space and resampled at 2 × 2 × 2 mm^3 voxel size. Normalized images were spatially smoothed using an 8-mm full-width at half-maximum Gaussian kernel to meet the statistical requirements of the general linear model and to compensate for residual macroanatomical variations.

Statistical Analysis

The fMRI data were analyzed using the general linear model as implemented in SPM5. The event-related modeling of experimental events (presentation of arrows) used a boxcar reference vector (width: 200 ms) convolved with a canonical hemodynamic response function and its first-order temporal derivative. Choosing this model in spite of the blocked nature of the task was crucial, even though the temporally narrow trial spacing necessitated by the task precluded a direct comparison between different trials (e.g., frequent vs. infrequent response side) within a task block. Modeling each trial as a separate event, however, allowed providing a value of the parametric modulators for each event (Fig. 2*E*). Hereby, we were able to construct regressors that modeled (smooth) adaptation and readaptation processes, which can be reliably assessed in spite of the low-pass filter invoked by the sluggish BOLD response. We included 3 parametric modulators of event-related activity into the experimental design:

1. The first modulator reflected whether a particular event required a left- or right-hand response. That is, whereas the main regressor should contain the activity present in any (left- or right-hand) response, side-specific activity should be captured by this first parametric modulator.
2. The second parametric modulator reflected the acquisition of a response bias at the start of a new block and was hence only computed for the first part of each block. First, we calculated, for each participant and trial, the difference in RT between right and left responses. After equalizing the direction of the RT differences across blocks (by inverting the values from blocks starting with 80% right-sided trials), the differences were averaged across all blocks from that participant. Lastly, we computed the absolute value of the first derivative of these RT differences. The ensuing vector describes, for each participant, the average development of response bias toward the more frequent side during the first part of each block. As

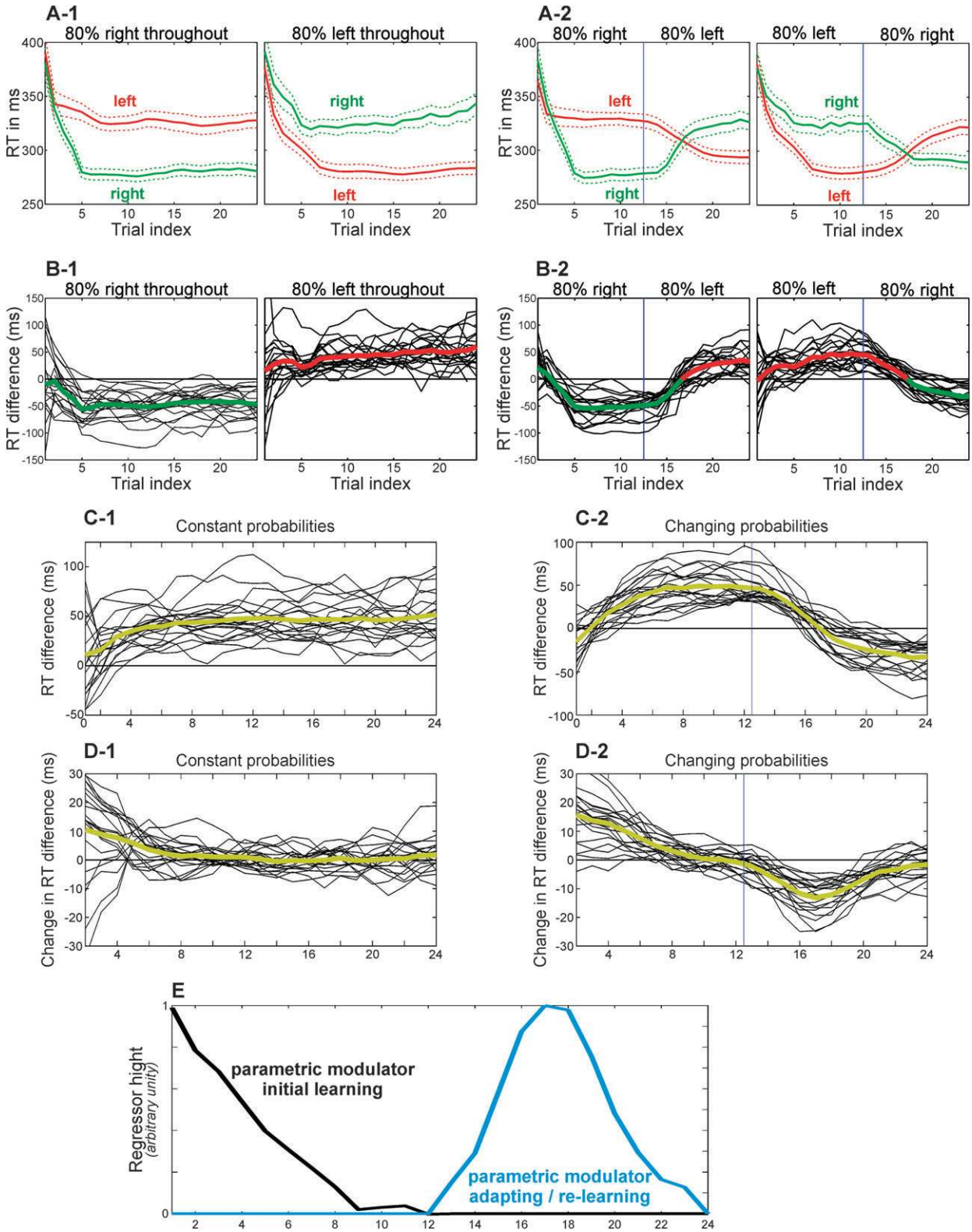

Figure 2. Behavioral results. (*A*) An RT advantage (mean RT ± standard error) was found for responses to high- versus low-probability stimuli, independent of response side, in blocks without probability reversal (NCC blocks; *A*-1) as well as in blocks with probability reversal (CC blocks; *A*-2). (*B*) Panels *B*-1 and *B*-2 depict group-averaged (colored) and individual mean RT differences between right- and left-response trials in NCC and CC blocks, respectively. (*C*) After multiplying the difference values from blocks starting with 80% right-sided trials by –1, these values were averaged across right- and left-response trials, separately for NCC (*C*-1) and CC (*C*-2) blocks. (*D*) The amount of trial-to-trial change in these RT differences was quantified by the first derivative of each difference score as shown in panels *D*-1 and *D*-2 for NCC and CC blocks, respectively. (*E*) Panel *E* shows the group average of the 2 parametric modulators, which were computed for each participant based on the averaged absolute values of the trial-to-trial change scores for the first half of NCC and CC blocks ("initial learning") as well as the second (postreversal) half of the CC blocks ("adapting/relearning").

participants start without any prior bias toward one side or the other, this change, that is, the integration of previous information into internal predictions, is particularly strong during the first couple of trials in each block (cf. behavioral results, Fig. 2). A positive effect on this modulator would thus be observed in brain regions that are most active at the beginning of a block, when prior knowledge cannot be used. In contrast, a negative effect would correspond to a region that becomes more active once information is gathered and predictions of the probabilistic structure can be employed by the participant to facilitate the most likely response.

3. The third modulator was used to model the period of adapting the previously acquired probability representations to the reversed probabilities in the second half of CC blocks. Specifically, this modulator reflects the change in response bias after the reversal of probabilities led to a prediction mismatch, driving the switch of the bias to the now more frequent side. This modulator was therefore only present in the second part of the CC blocks. We again computed, for each participant and CC block, the difference in RT between right and left responses, equalized the direction of the RT differences and averaged them across all blocks from that participant. Lastly, we again computed the absolute value of the first derivative of these RT differences. The ensuing vector describes, for each participant, the average change in response bias toward a given side, occurring from this trial to the next during the second part of CC blocks. As the vector takes an upward bell-shaped form (cf. behavioral results, Fig. 2) with maximum change of bias after a few trials into the second part, a positive effect would indicate regions becoming active during the process of adapting the current action predictions to the new probability distribution, driven by a strong prediction error. A negative effect, in turn, would be observed in regions suppressed during the change of expectations and relearning.

In sum, we used 3 parametric modulators: the first reflected response-side–specific activity (applied to both halves of each block); the second reflected bias acquisition at the beginning of a block (applied to the first half of each block); the third reflected bias reversal (applied to the second half of CC blocks). That is, the 2 latter modulators were only applied to those (nonoverlapping) periods of each CC and NCC block from which the underlying behavioral data were derived.

Low-frequency signal drifts were filtered using a cutoff period of 128 s. Parameter estimates were subsequently calculated for each voxel using weighted least squares to provide maximum likelihood estimators based on the temporal autocorrelation of the data (Kiebel and Holmes 2003). No global scaling was applied. For each subject, simple main effects for each experimental regressor (task condition and parametric modulations thereof) were computed by applying appropriate baseline contrasts. These individual first-level contrasts were then fed to a second-level group analysis using a random-effects analysis of variance (ANOVA; factor: condition; blocking factor: subject; Penny and Holmes 2003). In the modeling of variance components, we allowed for violations of sphericity by modeling nonindependence across images from the same subject and allowing unequal variances between conditions and subjects as implemented in SPM 5. Simple main effects of the task (vs. resting baseline) and the parametric modulators as well as comparisons between experimental factors were tested by applying appropriate linear contrasts to the ANOVA parameter estimates. Composite main effects (i.e., activations present in each of 2 different conditions) were tested by conjunction analyses (Nichols et al. 2005). Note that in spite of the fact that the parametric regressors should capture unique variance, the main regressor and its (orthogonal) modulators may still explain variance in the same brain region allowing for a significant effect in a conjunction analysis using the strict minimum statistic as employed here (Nichols et al. 2005). This is always the case if the fMRI signal can be modeled as a linear combination of a general signal increase during the presence of the task (main regressor) and an additional signal change conditioned on the state of the modulatory variable (parametric regressor). As all contrasts were based on *t*-statistics of the same ANOVA, the effective residual degrees of freedom = 76 (using the Satterthwaite approximation of the Greenhouse–Geisser correction for violations of the sphericity assumption) were identical for all comparisons. The resulting SPM(T) maps were then thresholded at $P < 0.05$ (cluster-level family-wise error-corrected; cluster-forming threshold at voxel-level $P < 0.001$; Worsley et al. 1996) and anatomically localized using version 1.5 of the SPM Anatomy toolbox (www.fz-juelich.de/ime/spm_anatomy_toolbox; Eickhoff et al. 2005, 2006, 2007).

Results

Behavioral Data

Debriefing after the experiment revealed that most participants did not notice a structure or bias in the stimulus presentation. Nevertheless, the behavioral data recorded in the scanner showed the typical advantage for the more frequent response. This is illustrated by the time course of mean RTs for responses to either side across the length of the NCC blocks (Fig. 2*A*). At the start of each NCC block, mean RT to stimuli on either side was close to 400 ms. Quickly, however, participants got into the rhythm of the serial stimulus presentation, and mean RT across both sides decreased to approximately 300 ms. This effect can be attributed to temporal preparation mechanisms, enabling participants to roughly (though not completely due to jittering) anticipate the occurrence of the next stimulus. Importantly, however, starting from the second event, RT for the frequent responses decreased considerably more than RT for the rare responses, leading to an RT advantage of about 50 ms. As shown in Figure 2*B*, the change of this behavioral advantage (i.e., the first derivative of the RT difference) was maximal after the first stimuli and decreased quickly. The change leveled out after about 7 trials, when the RT difference reached a plateau and remained constant throughout the rest of the block. The behavioral effects during NCC blocks can hence be summarized as follows: On top of an initial general RT decrease, presumably due to temporal preparation, there was a clear and quickly developing behavioral advantage for responding to the more frequent stimuli, which reached a plateau after about 7 trials at a difference of 50 ms.

A virtually identical response pattern was observed in the first part of the CC blocks. After the reversal of the stimulus probabilities in their second part, however, we observed a very clear behavioral change. RT toward the previously rare (20%) stimuli, which now occurred with a probability of 80%, quickly decreased, while RT to the previously more frequent stimuli started to increase. After approximately 5 trials under the new distribution, responses to either side became equally fast (RT $\approx$ 300 ms). Behavioral adaptation, however, did not stop at this equilibrium. Rather, the behavioral advantage was reversed after another 3 to 4 trials. By the end of the CC block, participants had completely changed their response bias and responded considerably ($\approx$ 30 ms) faster to the previously rare but now more frequent stimuli.

Error percentages mirrored the RT data: averaged across the first part of all blocks, low-probability trials incurred more errors (17%) than high-probability trials (3%). This bias remained constant in the second part of NCC blocks (low-probability trials: 21% errors; high-probability trials: 2%). In CC blocks, however, the bias in error percentage reversed in the second part in accord with the probability reversal (low-probability trials: 13%; high-probability trials: 5%). This somewhat reduced bias is again consistent with the RT data and presumably results from the shorter time available to establish the new bias during the second half of the CC blocks.

Imaging Data—Task-Related Activity

Compared with resting baseline, performance of the RT task per se, independent of any modulatory effects, recruited

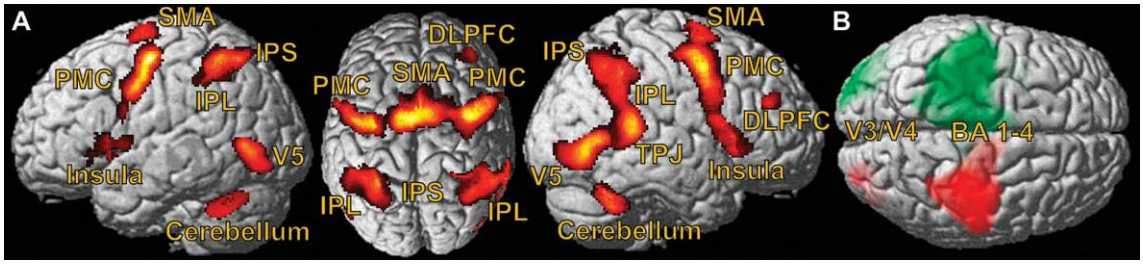

Figure 3. (*A*) Activations associated with performance of the 2-choice RT task (main task effect relative to resting baseline, independent of response side and behavioral effects reflected in respective parametric modulators). (*B*) Stimulus-side–specific activity captured by the first parametric regressor, shown separately for trials with left-pointing (red) or right-pointing (green) arrows. Displayed activations are significant at $P < 0.05$ (corrected at cluster level, voxel-wise inclusion threshold: $P < 0.001$). rDLPFC, right dorsolateral prefrontal cortex.

Table 1
Brain regions recruited during task performance

Location	Hemisphere	Histological assignment	*t*	MNI coordinates		
				x	*y*	*z*
SMA	Left	BA 6	12.02	−8	2	54
	Right	BA 6	8.07	8	−2	62
dPMC	Left	BA 6	9.32	−36	−9	50
	Right	BA 6	9.26	42	−5	56
vPMC	Left	BA 6	7.63	−47	−5	39
	Right	BA 6	7.83	42	0	41
	Right	BA 44/BA 6	6.21	43	3	27
Putamen	Left	—	7.28	−24	11	−5
	Right	—	6.86	21	8	5
Insula	Left	—	6.10	−36	18	6
	Right	—	7.41	32	21	9
DLPFC	Right	—	4.43	39	42	27
IPS	Left	hIP1-3/7A/7PC	9.86	−30	−51	51
	Right	hIP1-3/7A/7PC	7.61	30	−47	41
IPL	Left	PGa/PFm/PF	5.49	−51	−51	53
	Right	PGa/PFm	5.93	59	54	33
TPJ	Right	PFm	7.86	62	−42	11
Visual cortex	Left	hOC5 (V5)	7.56	−48	−74	0
	Right	hOC5 (V5)	7.16	47	−62	3
Cerebellum (lateral)	Left	Lobus VI/VIIa	7.83	−36	−51	−33
	Right	Lobus VI/VIIa	7.43	36	−54	−30
Cerebellum (medial)	Left	Lobus VI	6.44	−11	−75	−24
	Right	Lobus VI	6.27	8	−72	−18

Note: Histological assignment was based on probabilistic cytoarchitectonic maps as implemented in the SPM Anatomy Toolbox (Eickhoff et al. 2005, 2007). Significance level at $P < 0.05$ (corrected at cluster level, voxel-wise $P < 0.001$).

a widespread frontoparietal network (see Fig. 3*A* and Table 1). Dorsal and ventral premotor cortices (dPMC/Area 6 and vPMC/Areas 6 and 44; for cytoarchitectonic definitions, see Geyer 2004 and Amunts et al. 1999, respectively), the SMA (Area 6) as well as the parietal lobe, including the superior parietal lobule (SPL/Areas 7A and 7C; cf. Scheperjans, Eickhoff, et al. 2008; Scheperjans, Hermann, et al. 2008), the anterior parietal cortex (Area 2; cf. Grefkes et al. 2001), the IPS (Areas hIP1-3; cf. Choi et al. 2006; Scheperjans, Eickhoff, et al. 2008; Scheperjans, Hermann, et al. 2008), and the IPL (Areas PGa /PFm/PF; cf. Caspers et al. 2006, 2008), were bilaterally activated. The visual cortex (V5/hOc5; cf. Malikovic et al. 2007), the anterior insula, and the cerebellum (lobes IV–VIII) as well as the basal ganglia (putamen) were also activated bilaterally. Right-hemispheric activation was observed in the region of the temporoparietal junction (TPJ/Area PF; cf. Caspers et al. 2006, 2008) and the DLPFC.

Analyzing the modulatory effects of right- vs. left-hand responses as assessed by the first parametric regressor revealed the well-established network of contralateral primary motor (M1/Areas 4a and 4p; cf. Geyer et al. 1996) and somatosensory (S1/Areas 3b, 3a, 1, 2; cf. Geyer et al. 1999, 2000; Grefkes et al. 2001) cortices, which were accompanied by activation of the ipsilateral cerebellum (lobes IV, V, VII, VIII). Moreover, as the decisive part of the stimulus (arrowhead) was also lateralized, we also found significantly increased activation in contralateral visual cortex (V3v, V3d, V4, V3A, Area 17, and Area 18; cf. Amunts et al. 2000; Kujovic et al. 2007; Rottschy et al. 2007). Results are depicted in Figure 3*B*.

Imaging Data—Applying Learned Predictions

Areas related to the acquisition and application of implicit predictions about the probability structure of the stimuli and, hence, the required responses were delineated by testing for the second parametric modulator as described above. It reflected the first derivative of the absolute RT difference between left and right responses, that is, the change in response bias presumably generated by developing a prediction of upcoming events under decreasing entropy. The negative effect on this modulator tested for areas that became increasingly active once information about previous stimuli accumulated and predictions about upcoming events could be made based on this information. This analysis was further restrained to areas showing a significant main effect of the task per se by a conjunction approach. Significant results (see Fig. 4 and Table 2) were observed bilaterally in the IPL (mainly Area PFm, to a lesser degree areas PF and PGa) spreading into the IPS (Areas hIP1–3). Though present bilaterally, IPL activation was predominantly right lateralized, extending into right TPJ (Area PF). Additional effects were found in SMA (Area 6) and, on the right side, in dPMC and vPMC (comprising both Area 6 and Area 44) as well as the anterior-dorsal insula. All of these regions increased their activity when information from previous events was increasingly integrated into a behaviorally evident prediction of action probabilities, which could be used to facilitate the most frequently correct response.

There was, however, no significant positive modulation, testing for areas that were more active when the probabilistic structure was unknown and decreased in activity once prior knowledge could be used. Only at a considerably more liberal, uncorrected level ($P < 0.03$), activation was found in the right cerebellum (lobules VI and VIII).

Imaging Data—Dynamic Adaptation of Predictions

Areas related to behavioral adaptation, that is, relearning the reversed probability structure of stimuli and responses, were delineated by testing for the third parametric modulator as described above. This modulator reflects the absolute change in the RT difference between left and right responses during the second half of CC blocks, that is, the modulation of the response bias after the probability reversal (cf. Fig. 2). The positive modulation by this inversely *U*-shaped regressor tested

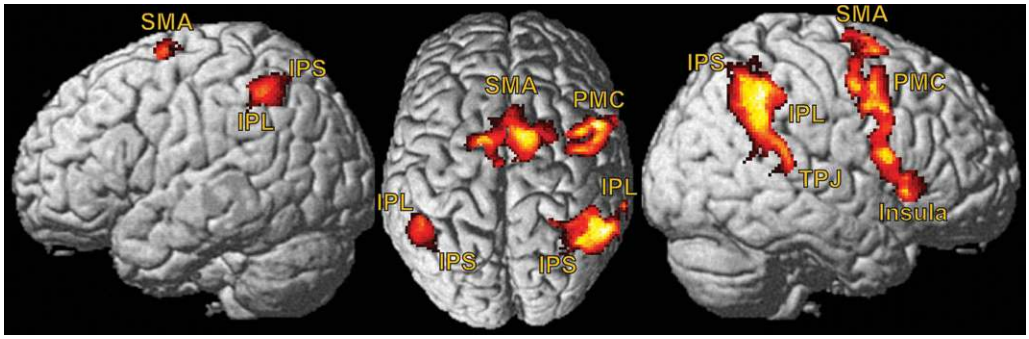

Figure 4. Brain areas presumably involved in the application of initially developed predictions (conjunction across task main effect and areas negatively associated with the second parametric regressor). Accumulated information on stimulus–response probabilities is used to establish selective facilitation, resulting in a response bias. Displayed activations are significant at $P < 0.05$ (corrected at cluster level, voxel-wise inclusion threshold: $P < 0.001$). For a list of abbreviations, see Figure 3.

Table 2
Brain activity correlated with the increasing application of learned predictions

Location	Hemisphere	Histological assignment	*t*	MNI coordinates		
				x	*y*	*z*
IPL	Left	PFm	5.30	−53	−46	58
	Right	PGa/PFm/PF	5.93	59	−54	33
TPJ	Right	PF	4.51	66	−36	12
IPS	Left	hIP 1–3	3.41	−50	−45	42
	Right	hIP1-3/7A/7PC	5.02	41	−50	45
vPMC	Right	BA 6	5.41	53	−3	47
	Right	BA 44	4.39	42	8	23
dPMC	Right	BA 6	4.24	42	6	53
Anterior insula	Right	—	4.61	36	20	−2
SMA	Left	BA 6	5.34	−5	2	65
	Right	BA 6	4.54	11	−3	69
Caudate nucleus	Left	—	4.60	−9	6	9

Note: Histological assignment was based on probabilistic cytoarchitectonic maps as implemented in the SPM Anatomy Toolbox (Eickhoff et al. 2005, 2007). Significance level at $P < 0.05$ (corrected at cluster level, voxel-wise $P < 0.001$).

for areas which first became increasingly active just after the probability reversal, when expectations needed to be adapted to produce an RT advantage for the opposite side, and which later on became less active again, when the relearning was finished and new predictions were established and applied successfully. This analysis was again restricted to areas showing a significant main effect of task execution per se. Significant results (see Fig. 5 and Table 3) were observed bilaterally in the SMA, dPMC (both Area 6), and IPS (predominantly hIP3). The latter activation also reached into SPL (Areas 7A/7PC) and IPL (Areas PF, PFm). During bias adaptation, right-lateralized activation was found in the TPJ (Areas PFm and PF) and the posterior part of the middle temporal gyrus (hOC5/V5). Finally, activation positively correlated with the dynamic reorganization of expectations was also found mainly on the right side of the anterior nuclei of the thalamus, basal ganglia (caudate nucleus, putamen) and the anterior-dorsal insula. No areas, however, were significantly negatively correlated with the behavioral adaptation, that is, showed reduced activity when the probabilistic structure changed in the CC blocks.

Imaging Data—Areas for Predictive Motor Coding

Finally, we aimed to identify brain areas related to employing and modifying predictions about the probability of specific events. This question is based on the concept that predictions are constantly evaluated against the current input. If the observed stimulus or response matches the prediction, it will be reinforced; if not, the prediction will be adapted to reflect environmental changes. To delineate regions serving this predictive coding, we performed a conjunction analysis across the 3 contrasts reported above (task main effects as well as second and third parametric modulators for establishing and readjusting predictions, respectively). This analysis revealed significant effects in the SMA (BA 6, bilaterally), the right IPS (Areas hIP 1–3, spreading into superior parietal areas 7A and 7PC), and right IPL (Areas PF/PFm). Further overlap just below the cluster-level corrected threshold ($P < 0.05$) was observed in the right dPMC (Area 6), DLPFC, and TPJ (Area PF) as well as in the left IPS and IPL (Areas hIP 1–3/PF, PFm). Results are presented in Figure 6 and Table 4.

Discussion

This study assessed the behavioral and neural effects of biased stimulus–response probabilities on choice RT performance in order to provide further insights into predictive-coding mechanisms in the context of speeded motor responses. Participants started each block naïve about the relative stimulus probabilities but quickly optimized their behavior as evidenced by an ≈50 ms RT advantage for the more frequent side. When the probabilities were inverted, the behavioral bias reversed within about 10 trials. The higher error rate for low-probability targets indicates that the observed RT shifts do not reflect a mere shift in the speed–accuracy tradeoff. Together, these data point to an efficient, highly flexible mechanism for predicting upcoming stimuli and facilitating the appropriate response.

The behavioral effects were associated with distinct patterns of neural activation. To account for interindividual differences in the time course of bias development and adaptation, fMRI analysis was based on assessing the modulation of neuronal activation by the subject-specific behavioral data. We showed that establishing/applying and modifying implicit predictions were correlated with increased activity in the parietal cortex (IPL/IPS), PMC (dPMC and SMA), DLPFC, and TPJ. Thus, predictive motor coding recruited a bilateral dorsal frontoparietal network as well as 2 ventral right-hemispheric areas (DLPFC and TPJ), which have previously been implicated in integrative, "higher" aspects of attention and motor control.

Response Biases, Predictive Motor Coding, and Information Theory

As an automated mechanism allowing the brain to structure the environment and prepare adequate motor responses (Friston 2002; Kilner et al. 2007; Jakobs et al. 2009), predictive motor

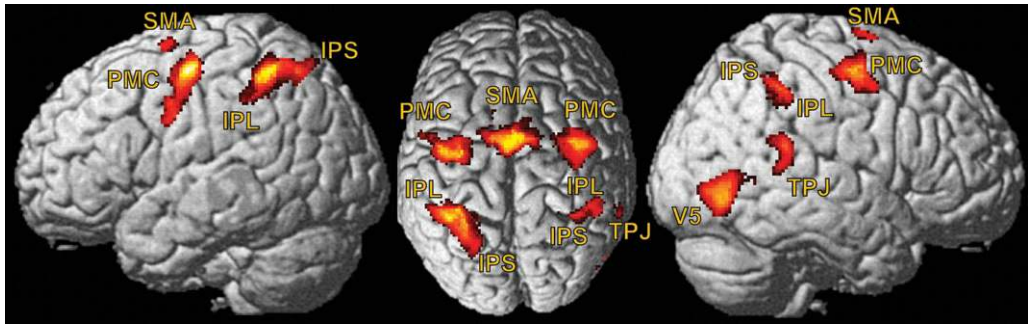

Figure 5. Brain areas presumably involved in the dynamic adaptation of predictions and change in response bias after the probability reversal (conjunction across task main effect and areas positively associated with the third parametric regressor). Amassing prediction errors lead to an update of existing predictions, thus generating a new, inverted response bias. Displayed activations are significant at $P < 0.05$ (corrected at cluster level, voxel-wise inclusion threshold: $P < 0.001$). For a list of abbreviations, see Figure 3.

Table 3
Brain activity correlated with the dynamic adaptation of predictions

Location	Hemisphere	Histological assignment	*t*	MNI coordinates		
				x	*y*	*z*
IPS	Left	hIP 3/7A/7PC	5.01	−24	−60	51
	Right	hIP 3/7A/7PC	4.75	29	−44	38
IPL	Left	PGa/PFm/PF	4.86	−48	−47	54
	Right	PGa/PFm/PF	3.98	47	−44	47
TPJ	Right	PF/PFm	4.86	56	−41	20
SMA	Left	BA 6	6.03	−6	−2	54
	Right	BA 6	4.55	8	−2	71
dPMC	Left	BA 6	5.58	−42	−12	56
	Right	BA 6	5.22	41	−8	51
Visual cortex	Right	hOC5 (V5)	6.00	47	−71	−3
Anterior insula	Left	—	4.51	−32	26	6
	Right	—	5.98	32	21	12
Putamen	Right	—	4.66	21	17	−2
	Left	—	4.20	−24	12	11
Thalamus	Right	—	5.88	17	−12	9
Caudate nucleus	Right	—	4.18	21	9	14

Note: Histological assignment was based on probabilistic cytoarchitectonic maps as implemented in the SPM Anatomy Toolbox (Eickhoff et al. 2005, 2007). Significance level at $P < 0.05$ (corrected at cluster level, voxel-wise $P < 0.001$).

coding does not depend on conscious awareness. This view is supported by the observation that our subjects, who were required to focus on responding as fast and correctly as possible to a rapid train of stimuli, did not report awareness of the biases when debriefed after scanning.

In our experiment, predictive coding appeared behaviorally advantageous as participants quickly developed faster responses to the predominant stimulus side. As no a priori information was available and short SOAs largely prohibited conscious anticipatory strategies, this implicit knowledge must have been gathered on-line via integration of previous events into a probabilistic model of expectations. Once established, this model would then entail the observed bias and faster reactions toward the more frequent, that is, predicted, side. Deviant stimuli, in turn, should necessitate longer response latencies due to reactive processing, as confirmed by our behavioral data. Additionally, they should evoke a higher prediction error indicating that the current model may no longer be valid. If amassing, these errors should trigger changes in the model structure to optimize future predictions, which is evident in the progression of RT after the probability reversal in CC blocks. In sum, the behavioral effects seen in the present experiment are well explained by the theory of predictive motor coding entailing the generation of a probabilistic model at the start of each block and a change thereof, driven by amassing prediction errors, in the second part of the CC blocks.

A recent study using transcranial magnetic stimulation (TMS) showed that 2 information-theoretic measures related to probabilistic structure in a task, entropy and surprise, are associated with the excitability of the motor pathway during preparation for speeded action (Bestmann et al. 2008). In this framework, entropy reflects the average uncertainty about a given motor response, whereas surprise reflects the improbability of the occurrence of a particular response cue (cf. Strange et al. 2005). For instance, when 2 alternative responses are equally probable, entropy is maximal but the surprise at the occurrence of either alternative is at an intermediate level. When unequal probabilities reduce entropy (i.e., enhance predictability), surprise at occurrence of the more probable alternative decreases at the expense of an increase in surprise when the less probable alternative occurs. This entails an important distinction between the 2 measures: entropy is independent of the current event but reflects the context established by previous events. In contrast, surprise refers to the evaluation of the current event against expectations based on the current entropy level (Strange et al. 2005). This view effectively is a restatement, in quantifiable information-theoretic terms, of the long-established differentiation between the endogenous, expectancy-driven and exogenous, stimulus-driven orienting of attention (cf. Corbetta and Shulman 2002).

In terms of information theory, predictive motor coding should be subserved by regions that use decreasing entropy (i.e., increasing predictability) to develop and represent unconscious expectations (i.e., attentional biases). Given the current data, we would argue for a role of the regions revealed by the "applying learned predictions" contrast in these processes. In particular, while the TPJ may represent a measure of entropy (cf. Jakobs et al. 2009), the IPS and premotor cortex may represent the ensuing expectations. Evidently, this process also entails a growing difference in surprise associated with the occurrence of the more and less likely alternative, respectively, which is reflected well in our behavioral data. After the probability reversal (which represents no objective change in entropy as the average uncertainty remains constant), amassing prediction errors are reduced by giving more weight to bottom-up sensory input. This effectively equals a subjective increase in entropy, which is then reduced again over the further course of the block by the development of a new

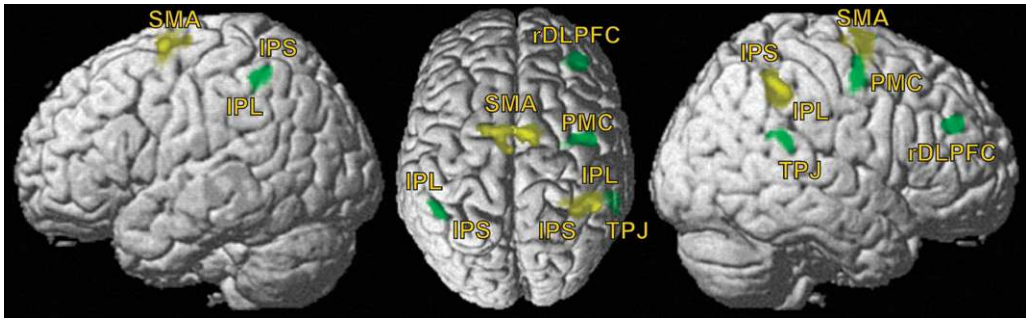

Figure 6. Core regions of a network subserving predictive motor coding, that is, brain areas presumably involved in both the application of initially developed predictions and the dynamic adaptation of existing predictions after the probability reversal (conjunction across task main effect, areas negatively associated with the second parametric regressor, and areas positively associated with the third parametric regressor). Yellow denotes common activations significant at $P < 0.05$ (corrected at cluster level, voxel-wise inclusion threshold: $P < 0.001$); green denotes activations significant at: $P < 0.001$ (voxel-wise, $k = 175$ voxels). For abbreviations, see Figure 3.

Table 4
Brain areas involved in the computation of predictive motor coding

Location	Hemisphere	Histological assignment	*t*	MNI coordinates		
				x	*y*	*z*
SMA	Left	BA 6	4.37	−18	0	66
	Right	BA 6	4.27	9	−2	71
IPS	Right	hIP 1–3/7A/7PC	4.32	41	−42	44
IPL	Right	PFm/PF	3.98	47	−44	47
dPMC*	Right	BA 6	4.55	47	−6	53
DLPFC*	Right	—	4.21	38	41	29
TPJ*	Right	PF	4.50	57	−41	21
IPL*	Left	PFm/PF	4.06	−47	−50	53
IPS*	Left	hIP 1–3	3.98	−50	−45	51

Note: Histological assignment was based on probabilistic cytoarchitectonic maps as implemented in the SPM Anatomy Toolbox (Eickhoff et al. 2005, 2007). Significance level at $P < 0.05$ (corrected at cluster level, voxel-wise $P < 0.001$). *, uncorrected for multiple comparisons (voxel-level $P < 0.001$; $k = 175$ voxel).

expectation. Importantly, the results of our conjunction across both bias establishment and bias reversal are largely consistent with a network associated with stimulus-bound surprise identified by Strange et al. (2005) using a visual 4-choice RT task with unequal response probabilities. The congruence of these and our results with the ventral attention network (cf. Corbetta and Shulman 2002) finally attests to the conceptual overlap between surprise, reactive processing and the orienting of attention to unexpected stimuli (see also Corbetta et al. 2008).

Brain Areas Implicated in Predictive Mechanisms

IPS and IPL

Bilateral activations of the IPS and IPL throughout all conditions imply a central role of these regions in the implementation of predictions in sensorimotor processing. In a recent review, Creem-Regehr (2008) concluded that this region is responsible for generating internal representations for action, which may also contain probabilistic information as evident from our data. In fact, a study in nonhuman primates found neurons in the lateral IPS coding the hazard rate, that is, the conditional probability of stimulus/response occurrence (Janssen and Shadlen 2005). Also, studies on patients with IPL and TPJ lesions revealed a role of these areas in producing spatial and temporal biases in sensorimotor processing, suggesting a role in the selection among competing targets for motor acts (Ro et al. 2001; Shapiro et al. 2002). Thus, rising parietal activity over the first half of a block may reflect the growing bias in the representation of potential forthcoming actions. This also agrees with the finding in nonhuman primates that IPS neurons code action intentions (Snyder et al. 1997, 1998). Our data now suggest that these signals may not only represent categorical intentions (Mattingley et al. 1998) but also the probability of their implementation and the associated bias in sensorimotor processing.

Moreover, the parietal lobe has also been implicated in attentional modulation of sensory processing (Corbetta and Shulman 2002; Balan and Gottlieb 2006; Vandenberghe and Gillebert 2009). This includes orienting to relevant environmental stimuli (Corbetta and Shulman 2002) and shifting or reengaging attention (Balan and Gottlieb 2006; Corbetta et al. 2008). Therefore, the observed IPS/IPL finding in our study may relate to an increased bottom-up–driven reorienting of attention attracted by the nonpredicted arrow (cf. Fletcher and Frith 2009 for a discussion of the relationship between prediction error of attention).

SMA

As the SMA is known to be involved in movement preparation and initiation (Jenkins et al. 2000; Thickbroom et al. 2000; Cunnington et al. 2003), its computations should primarily concern the kinematics level and patterns of muscle coordination of a movement. Using internal predictions, these may partially be executed in advance, leading to a decrease of computational load at the moment of execution and hence faster movement initiation, that is, lower RT.

Miller (1998) used electroencephalography (EEG) to measure lateralized readiness potentials (LRPs or "Bereitschaftspotential") during the performance of a 2-choice RT task with unequal probabilities; he observed enhanced LRPs in high-probability trials. Based on the temporal relation of this effect relative to stimulus offset and motor responses, he concluded that the probability effect is facilitated, at least partly, by motor preparatory processes. In line with the current view of the SMA as the generator of the LRP (Deecke and Kornhuber 1978; Nachev et al. 2008), we would conclude that Miller's (1998) observations as well as our own results indicate a precomputation of the predicted movement within the SMA. In the hierarchical framework of predictive motor coding (Kilner et al. 2007), SMA would thus correspond to a lower-level node generating predictions about kinematical movement features. Consequently, increased SMA activity concurrent with the

development of the behavioral bias should reflect the preponderance to prepare motor programs once a probabilistic structure is learned. On the other hand, its recruitment during the adaptation process would correspond to the modulation or exchange of these prepared kinematical programs.

TPJ

Several studies suggested TPJ involvement in the stimulus-driven reorienting of visual attention (Serences et al. 2005; Yeh et al. 2007; Shulman et al. 2009). Corbetta and Shulman (2002) proposed that TPJ activity is related to breaches of expectancy (i.e., surprise) due to unexpected but behaviorally relevant stimuli. This notion agrees with findings in our experiment where task performance depends not only on preparing responses to the more likely alternative but also on the ability to reorient attention to unexpected events. Evidently surprise and importance for deviance detection are dependent on the establishment of a predictive model, which explains why at the beginning of each block, TPJ activity increases in parallel with the behavioral bias.

Higher TPJ activity was also observed during the adaptation of predictions in the wake of the probability reversal where the breach of expectations may have enforced more reactive response processing including attentional reorientation (Kincade et al. 2005; Jakobs et al. 2009). It has moreover been argued that such reorientation would be triggered by the presence of a higher prediction error (Mackintosh 1975; Pearce and Hall 1980) providing a predictive coding framework for the stimulus-driven reallocation of attentional resources (Fletcher and Frith 2009). In summary, we would thus conclude that the TPJ may relate to detecting and processing unexpected stimuli, which would be in line with lower activity at the start of a block before the formation of a prediction and higher activity after probability reversal when most incoming information does not match the expectation. Whether, however, attentional reorientation or prediction error signaling may be differentiated and if so, which role the TPJ plays in processing either, needs to remain open for now.

dPMC and DLPFC

There is converging evidence from neuroimaging, lesion analysis, and TMS interventions showing that the dPMC plays a crucial role in motor planning, especially in integrating visual input relevant for forthcoming motor commands and maintaining the stimulus–response mapping (Halsband and Passingham 1985; Chouinard et al. 2005; Chouinard and Paus 2006). Hoshi and Tanji (2007) more specifically argued that dPMC collects and integrates sensory and memory information to establish action intentions and develop the respective motor programs. This view is supported by primate data showing that the dPMC (Area F2) is involved in preparing movements based on sensorimotor information and behavior-guiding rules (Rizzolatti et al. 1998; Luppino et al. 2003). We suggest that increased activity of the dPMC in the first half of each block as well as after probability reversal in the current study reflects a modulation of the stimulus–response mapping according to the current prediction, facilitating the predicted response.

This conclusion regarding the integration of lower-level sensorimotor and higher-level contextual information in dPMC for selecting (or preparing) the correct motor response from available stimulus–response mappings is also consistent with the hierarchical cascade model of cognitive control recently proposed by Koechlin and Summerfield (2007). In this framework, sensorimotor associations are maintained in dPMC; their application to produce appropriate motor output, however, is influenced by context information represented in DLPFC.

Recent studies have supported a role for the DLPFC in response selection (Hadland et al. 2001; Rowe et al. 2008; Wang et al. 2009), acting as a filter for task-appropriate responses (Mostofsky and Simmonds 2008). This proposal is also in line with studies using the go/no-go paradigm (Nakata et al. 2008; Yamaguchi et al. 2008), which found DLPFC activation when a prepotent response needed to be inhibited. Consistent with Koechlin and Summerfield's (2007) cascade model of cognitive control, which conceptualized the role of the anterior DLPFC as providing contextual information for response selection, we found activity related to bias development and readaptation in this region. The context coded by anterior DLPFC activity might thus include information, accumulated over previous trials, on the predictability (i.e., average entropy) and probability of a given outcome. In light of this theorizing, the course of DLPFC activity during the acquisition and modification of stimulus–response probabilities may suggest that this region receives probability estimations and error signals from posterior regions, which it represents to provide executive control over the implementation of motor output.

Cerebellum and Further Activations

While the above-mentioned regions were commonly activated by the task per se as well as by the acquisition and modification of stimulus–response probabilities, several other regions were selectively associated with one of these components. For instance, medial and lateral parts of the cerebellum (lobules VI and VII) were significantly activated during task execution. Given the employed jittered stimulus presentation, this finding is consistent with previous evidence that the posterior cerebellum (lobules VI/VII and crus 1) operates as an internal timing system, providing precise temporal representations (Sakai et al. 2000; Dreher and Grafman 2002). Contrarily to our hypothesis, however, generating and updating predictions did not produce an increased activation of this region, although cerebellar contributions have been extensively discussed in the context of sensorimotor predictions (Miall et al. 1993), error detection (Oscarsson 1980), and predictive learning (Wolpert and Kawato 1998; Schultz and Dickinson 2000). It has been suggested, however, that the predictive functions of the cerebellum are more related to emulating sensory consequences of motor actions and comparing these with actual proprioceptive input (Blakemore and Sirigu 2003). Since these processes are constantly invoked in all trials, they provide another explanation for the association of this structure with the task per se as well as for the lack of cerebellar involvement in the establishment and adaptation of specific biases in perceptual-motor predictions.

A significant rise in basal ganglia activity was selectively observed when participants adapted their predictions following the probability reversal. Several studies have shown that the basal ganglia react specifically to task order unpredictability (Dreher and Grafman 2002) or to unexpected attentional shifts (Shulman et al. 2009). The observed basal ganglia activity therefore appears to relate to the surprising change in the environment and thus response requirements. These conclusions match recent results by Den Ouden et al. (2009), who reported that the putamen is

sensitive to surprising events and unexpected outcomes and interpreted this finding as a reflection of prediction errors. As prediction errors should be particularly prevalent after the probability reversal, we support this interpretation and suggest that the adjustment of the response bias should be driven by error signals generated in this structure.

Activity of right BA 44 during task performance per se is in line with the notion that this area may serve as an "executive brake" when stimulus timing is unknown and hence action needs to be inhibited until stimulus presentation (Brass et al. 2005; Chambers et al. 2006; Jakobs et al. 2009). As we employed jittering of the stimuli, prepared responses needed to be withheld while waiting for the expected arrow to prevent premature responding (cf. Konishi et al. 1999). Moreover, the need to withhold premature responses should increase with increased preparation according to more firmly established predictions. This may explain the increase in BA 44 recruitment throughout the course of each block in parallel with increased bias.

The anterior insula was involved in both task execution and adaptation of predictions. This region is known to be involved in representing bodily states (Craig 2002; Critchley et al. 2004) and arousal induced by mental or physical stressors (Critchley et al. 2000; Pollatos et al. 2007). Thus, general task-related activity may be related to maintaining an appropriate level of alertness, whereas the association of insula activity with prediction adjustment might point to the long-known association between surprise and arousal (for a recent review, see Pfaff 2006).

Finally, activity in visual area V5 during general task execution is in good agreement with the known responsiveness of this region to moving or flickering/blinking stimuli (Zeki et al. 1991; Jantzen et al. 2005; Grefkes et al. 2008). Although this activity appeared right lateralized, we found additional left-hemisphere V5 activity just below the corrected threshold. Moreover, our results show V5 recruitment after the probability reversal, which may be linked to an attentional modulation of visual processing under increased uncertainty due to invalidated predictions (Corbetta et al. 1990; O'Craven et al. 1997).

Limitations and Further Directions

The temporally narrow spacing of the trials, necessary for pushing participants into biasing their responding according to implicit predictions, unfortunately precluded a direct comparison between different trials (e.g., correct vs. errors trials) within a task block. Likewise, sequential effects reflecting the effect of the preceding trial on the processing during the current trial could not be analyzed. Longer intertrial intervals, however, might have increased the likelihood of participants becoming aware of the probability structure and deploy explicit, conscious strategies rather than implicit expectations. Consequently, we restricted our analysis to the evaluation of the (smooth) adaptation and readaptation processes, which can be reliably assessed in spite of the low-pass filter invoked by the sluggish BOLD response.

As mentioned before, the third parametric modulator reflected 2 subprocesses of bias reversal: removal of the existing bias ("bias debuilding") and implementation of the reversed bias ("bias rebuilding" or readaptation). The limitations inherent to fMRI, however, appear to prohibit separate analyses of the potentially different neural correlates thereof. On the one hand, the number of data points reflecting bias removal only consists of a few images per block, putting any inference on unreliable ground. On the other hand, and even more importantly, a statistical separation of these 2 processes in fMRI data is not feasible at present because bias readaptation inevitably directly follows bias removal without any chance to randomize their order or to introduce a (variable and/or sufficiently long) interval between them. Their convolution with the hemodynamic response function acting as a low-pass filter would thus be essentially collinear. Therefore, disentangling the contribution of either subprocess to the sluggish BOLD response during the major part of the second half of CC blocks is statistically impossible. Moreover, since predictive motor coding is conditioned upon a fast stimulus presentation to avoid conscious preparation and explicit strategies, increasing separability by prolonging the interstimulus interval is precluded by the nature of the process under scrutiny. Consequently, identifying distinct neural correlates of either subprocess may depend on using imaging modalities with higher time resolution such as MEG or EEG.

It should be noted that the present experiment used a rather strongly biased probability distribution (20% vs. 80%), and it remains to be investigated to what extent the network discussed above would react parametrically to the size of the bias. Likewise, the influence of hyperpriors on the volatility of the environment (Behrens et al. 2007) also warrants further investigation. In particular, it may be speculated that the behavioral and neural bias may be attenuated once several probability reversals have been presented in the same block.

The question whether the probability effect is more related to biases at perceptual, response selection, or motor stages of the reaction process has been discussed previously without consensus. Some studies spoke for a perceptual locus (Bertelson and Tisseyre 1966; LaBerge et al. 1969), while a more recent study (Miller 1998) provided evidence for selective motor preparation. Our data suggest that all processing stages may be affected by unequal probabilities, since we found probability effects in areas related to perception (V5), response selection (IPS, IPL, DLPFC), and motor preparation (SMA, dPMC). It remains to be tested whether the contributions of these different components may be segregated.

Conclusions

This study investigated effects of unequal stimulus probabilities on brain activity during 2-choice RT task performance, showing that high-probability stimuli were responded too faster and more correctly, while this bias became inverted after a covert probability reversal. Within the theoretical framework of predictive coding, such biases can be explained by a constant adjustment of internal predictions about forthcoming actions to the observed environment at different hierarchical levels, affecting both perceptual and motor stages of the reaction process. Our study revealed several brain regions associated with the dynamic change of the response bias: TPJ may act as a detector for unpredicted but relevant low-probability stimuli by integrating predictions with sensory input. IPS and IPL may form a center for generating prediction-dependent action representations. In turn, biases in stimulus–response mapping, kinematic preparation, and the executive control thereof may be attributed to the dPMC, SMA, and DLPFC, respectively. To sum up, the association of these areas' activity level with parametric indices of probability-related behavior provides

strong evidence for their involvement in generating flexible, context-dependent response biases. They may thus form the core nodes of a network that mediates the generation of predictive motor codes and their transformation into selective action facilitation.

Funding

Human Brain Project (R01-MH074457-01A1 to S.B.E.); the Initiative and Networking Fund of the Helmholtz Association within the Helmholtz Alliance on Systems Biology (Human Brain Model to K.Z., S.B.E.), the Deutsche Forschungsgemeinschaft (IRTG 1328 to S.B.E.); and the Helmholtz Alliance for Mental Health in an Aging Society (HelMA to K.Z.).

Notes

Conflict of Interest: None declared.

References

Amunts K, Malikovic A, Mohlberg H, Schormann T, Zilles K. 2000. Brodmann's areas 17 and 18 brought into stereotaxic space—where and how variable? Neuroimage. 11:66–84.

Amunts K, Schleicher A, Bürgel U, Mohlberg H, Uylings HBM, Zilles K. 1999. Broca's region revisited: cytoarchitecture and intersubject variability. J Comp Neurol. 412:319–341.

Ashburner J, Friston KJ. 2003. Rigid body registration. In: Frackowiak RS, Friston KJ, Frith CD, Dolan RJ, Price CJ, Ashburner J, Penny WD, Zeki S, editors. Human brain function. 2nd ed. London: Academic Press. p. 635–655.

Balan PF, Gottlieb J. 2006. Integration of exogenous input into a dynamic salience map revealed by perturbing attention. J Neurosci. 26:9239–9249.

Behrens TE, Woolrich MW, Walton ME, Rushworth MF. 2007. Learning the value of information in an uncertain world. Nat Neurosci. 10:1214–1221.

Bertelson P, Tisseyre F. 1966. Choice reaction time as a function of stimulus versus response relative frequency of occurrence. Nature. 212:1069–1107.

Bestmann S, Harrison LM, Blaneknburg F, Mars RB, Haggard P, Friston KJ, Rothwell JC. 2008. Influence of uncertainty and surprise on human corticospinal excitability during preparation for action. Curr Biol. 18:775–780.

Blackman AR. 1972. Influence of stimulus and response probability on decision and movement latency in a discrete choice reaction task. J Exp Psychol. 92:128–133.

Blakemore SJ, Sirigu A. 2003. Action prediction in the cerebellum and in the parietal lobe. Exp Brain Res. 153:239–245.

Brass M, Derrfuss J, von Cramon DY. 2005. The inhibition of imitative and overlearned responses: a functional double dissociation. Neuropsychologia. 43:89–98.

Casey BJ, Forman SD, Franzen P, Berkowitz A, Braver TS, Nystrom LE, Thomas KM, Noll DC. 2001. Sensitivity of prefrontal cortex to changes in target probability: a functional MRI study. Hum Brain Mapp. 13:26–33.

Caspers S, Eickhoff SB, Geyer S, Scheperjans F, Mohlberg H, Zilles K, Amunts K. 2008. The human inferior parietal lobule in stereotaxic space. Brain Struct Funct. 212:481–495.

Caspers S, Geyer S, Schleicher A, Mohlberg H, Amunts K, Zilles K. 2006. The human inferior parietal cortex: cytoarchitectonic parcellation and interindividual variability. Neuroimage. 33:430–448.

Chambers CD, Bellgrove MA, Stokes MG, Henderson TR, Garavan H, Robertson IH, Morris AP, Mattingley JB. 2006. Executive "brake failure" following deactivation of human frontal lobe. J Cogn Neurosci. 18:444–455.

Choi H-J, Zilles K, Mohlberg H, Schleicher A, Fink GR, Armstrong E, Amunts K. 2006. Cytoarchitectonic identification and probabilistic mapping of two distinct areas within the anterior ventral bank of the human intraparietal sulcus. J Comp Neurol. 495:53–69.

Chouinard PA, Leonard G, Paus T. 2005. Role of the primary motor and dorsal premotor cortices in the anticipation of forces during object lifting. J Neurosci. 25:2277–2284.

Chouinard PA, Paus T. 2006. The primary motor and premotor areas of the human cerebral cortex. Neuroscientist. 12:143–152.

Corbetta M, Miezin FM, Dobmeyer S, Shulman GL, Petersen SE. 1990. Attentional modulation of neural processing of shape, color, and velocity in humans. Science. 24:1556–1559.

Corbetta M, Patel G, Shulman GL. 2008. The reorienting system of the human brain: from environment to theory of mind. Neuron. 58:306–324.

Corbetta M, Shulman GL. 2002. Control of goal-directed and stimulus-driven attention in the brain. Nat Rev Neurosci. 3:201–215.

Courville AC, Daw ND, Touretzky DS. 2006. Bayesian theories of conditioning in a changing world. Trends Cogn Sci. 10:294–300.

Craig AD. 2002. How do you feel? Interoception: the sense of the physiological condition of the body. Nat Rev Neurosci. 3:655–666.

Creem-Regehr SH. 2008. Sensory-motor and cognitive functions of the human posterior parietal cortex involved in manual actions. Neurobiol Learn Mem. 91:166–171.

Critchley HD, Corfield DR, Chandler MP, Mathias CJ, Dolan RJ. 2000. Cerebral correlates of autonomic cardiovascular arousal: a functional neuroimaging investigation in humans. J Physiol. 523(Pt 1):259–270.

Critchley HD, Wiens S, Rotshtein P, Öhman A, Dolan RJ. 2004. Neural systems supporting interoceptive awareness. Nat Neurosci. 7:189–195.

Cunnington R, Windischberger C, Deecke L, Moser E. 2003. The preparation and readiness for voluntary movement: a high-field event-related fMRI study of the Bereitschafts-BOLD response. Neuroimage. 20:404–412.

Deecke L, Kornhuber HH. 1978. An electrical sign of participation of the mesial 'supplementary' motor cortex in human voluntary finger movement. Brain Res. 159:473–476.

Den Ouden HE, Friston KJ, Daw ND, McIntosh AR, Stephan KE. 2009. A dual role for prediction error in associative learning. Cereb Cortex. 19:1175–1185.

Dreher J-C, Grafman J. 2002. The roles of the cerebellum and basal ganglia in timing and error prediction. Eur J Neurosci. 16:1609–1619.

Eickhoff SB, Heim S, Zilles K, Amunts K. 2006. Testing anatomically specified hypotheses in functional imaging using cytoarchitectonic maps. Neuroimage. 32:570–582.

Eickhoff SB, Paus T, Caspers S, Grosbras MH, Evans AC, Zilles K, Amunts K. 2007. Assignment of functional activations to probabilistic cytoarchitectonic areas revisited. Neuroimage. 36:511–521.

Eickhoff SB, Stephan KE, Mohlberg H, Grefkes C, Fink GR, Amunts K, Zilles K. 2005. A new SPM toolbox for combining probabilistic cytoarchitectonic maps and functional imaging data. Neuroimage. 25:1325–1335.

Fletcher PC, Frith CD. 2009. Perceiving is believing: a Bayesian approach to explaining the positive symptoms of schizophrenia. Nat Rev Neurosci. 10:48–58.

Friston K. 2002. Functional integration and inference in the brain. Prog Neurobiol. 68:113–143.

Friston K, Kiebel S. 2009. Cortical circuits for perceptual inference. Neural Netw. 22:1093–1104.

Friston K, Kilner J, Harrison L. 2006. A free energy principle for the brain. J Physiol Paris. 100:70–87.

Geyer S. 2004. The microstructural border between the motor and the cognitive domain in the human cerebral cortex. Adv Anat Embryol Cell Biol. 174:1–92.

Geyer S, Ledberg A, Schleicher A, Kinomura S, Schormann T, Bürgel U, Klingberg T, Larsson J, Zilles K, Roland PE. 1996. Two different areas within the primary motor cortex of man. Nature. 382:805–807.

Geyer S, Schleicher A, Zilles K. 1999. Areas 3a, 3b, and 1 of human primary somatosensory cortex. Neuroimage. 10:63–83.

Geyer S, Schormann T, Mohlberg H, Zilles K. 2000. Areas 3a, 3b, and 1 of human primary somatosensory cortex. Part 2. Spatial normalization to standard anatomical space. Neuroimage. 11:684–696.

Grefkes C, Eickhoff SB, Nowak DA, Dafotakis M, Fink GR. 2008. Dynamic intra- and interhemispheric interactions during unilateral

and bilateral hand movements assessed with fMRI and DCM. Neuroimage. 41:1382–1394.
Grefkes C, Geyer S, Schormann T, Roland P, Zilles K. 2001. Human somatosensory area 2: observer-independent cytoarchitectonic mapping, interindividual variability, and population map. Neuroimage. 14:617–631.
Hadland KA, Rushworth MF, Passingham RE, Jahanshahi M, Rothwell JC. 2001. Interference with performance of a response selection task that has no working memory component: an rTMS comparison of the dorsolateral prefrontal and medial frontal cortex. J Cogn Neurosci. 13:1097–1108.
Halsband U, Passingham RE. 1985. Premotor cortex and the conditions for movement in monkeys (Macaca fascicularis). Behav Brain Res. 18:269–277.
Heuer H. 1982. Choice between finger movements of different and identical form: the effect of relative signal frequency. Psychol Res. 44:323–342.
Holmes CJ, Hoge R, Collins L, Woods R, Toga AW, Evans AC. 1998. Enhancement of MR images using registration for signal averaging. J Comput Assist Tomogr. 22:324–333.
Hoshi E, Tanji J. 2007. Distinctions between dorsal and ventral premotor areas: anatomical connectivity and functional properties. Neurobiology. 17:234–242.
Jakobs O, Wang LE, Dafotakis M, Grefkes C, Zilles K, Eickhoff SB. 2009. Effects of timing and movement uncertainty implicate the temporo-parietal junction in the prediction of forthcoming motor actions. Neuroimage. 47:667–677.
Janssen P, Shadlen MN. 2005. A representation of the hazard rate of elapsed time in macaque area LIP. Nat Neurosci. 8:234–241.
Jantzen KJ, Steinberg FL, Kelso JA. 2005. Functional MRI reveals the existence of modality and coordination-dependent timing networks. Neuroimage. 25:1031–1042.
Jenkins H, Jahanshahi M, Jueptner M, Passingham RE, Brooks DJ. 2000. Self-initiated versus externally triggered movements II. The effect of movement predictability on regional cerebral blood flow. Brain. 123:1216–1228.
Kiebel S, Holmes AP. 2003. The general linear model. In: Frackowiak RS, Friston KJ, Frith CD, Dolan RJ, Price CJ, Ashburner J, Penny WD, Zeki S, editors. Human brain function. 2nd ed. London: Academic Press. p. 725–760.
Kilner JM, Friston KJ, Frith CD. 2007. Predictive coding: an account of the mirror neuron system. Cogn Process. 8:159–166.
Kincade JM, Abrams RA, Astafiev SV, Shulman GL, Corbetta M. 2005. An event-related functional magnetic resonance imaging study of voluntary and stimulus-driven orienting of attention. J Neurosci. 25:4593–4604.
Koechlin E, Summerfield C. 2007. An information theoretical approach to prefrontal executive function. Trends Cogn Sci. 11:229–235.
Konishi S, Nakajima K, Uchida I, Kikyo H, Kameyama M, Miyashita Y. 1999. Common inhibitory mechanism in human inferior prefrontal cortex revealed by event-related functional MRI. Brain. 122(Pt 5):981–991.
Kujovic M, Malikovic A, Schleicher A, Rottschy C, Eickhoff SB, Mohlberg H, Hömke L, Zilles K, Amunts K. 2007. Observer-independent cytoarchitectonic mapping of the dorsal extrastriate human visual cortex. 13th International Conference on Functional Mapping of the Human Brain; 2007 June 10–14; Chicago (IL): Elsevier. Abstract available on CD-ROM in NeuroImage 36(S1).
LaBerge D, Legrand R, Hobbie RK. 1969. Functional identification of perceptual and response biases in choice reaction time. J Exp Psychol. 79:295–299.
Laming DRJ. 1969. Subjective probability in choice-reaction experiments. J Math Psychol. 6:81–120.
Lungu OV, Wächter T, Liu T, Willingham DT, Ashe J. 2004. Probability detection mechanisms and motor learning. Exp Brain Res. 159:135–150.
Luppino G, Rozzi S, Calzavara R, Matelli M. 2003. Prefrontal and agranular cingulated projections to the dorsal premotor areas F2 and F7 in the macaque monkey. Eur J Neurosci. 17:559–578.
Mackintosh NJ. 1975. A theory of attention: variations in associability of stimuli with reinforcement. Psychol Rev. 82:276–298.
Malikovic A, Amunts K, Schleicher A, Mohlberg H, Eickhoff SB, Wilms M, Palomero-Gallagher N, Armstrong E, Zilles K. 2007. Cytoarchitectonic analysis of the human extrastriate cortex in the region of V5/MT+: a probabilistic, stereotaxic map of area hOc5. Cereb Cortex. 17:562–574.
Mattingley JB, Husain M, Rorden C, Kennard C, Driver J. 1998. Motor role of human inferior parietal lobe revealed in unilateral neglect patients. Nature. 392:179–182.
Miall RC, Weir DJ, Wolpert DM, Stein JF. 1993. Is the cerebellum a Smith predictor? J Mot Behav. 25:203–216.
Miller J. 1998. Effects of stimulus–response probability on choice reaction time: evidence from the lateralized readiness potential. J Exp Psychol Hum Percept Perform. 24:1521–1534.
Mostofsky SH, Simmonds DJ. 2008. Response inhibition and response selection: two sides of the same coin. J Cogn Neurosci. 20:751–761.
Nachev P, Kennard C, Husain M. 2008. Functional role of the supplementary and pre-supplementary motor areas. Neuroscience. 9:856–869.
Nakata H, Sakamoto K, Ferretti A, Perrucci MG, Del Gratta C, Kakigi R, Romania GL. 2008. Somato-motor inhibitory processing in humans: an event-related functional MRI study. Neuroimage. 39:1858–1866.
Nichols T, Brett M, Andersson J, Wager T, Poline JB. 2005. Valid conjunction inference with the minimum statistic. Neuroimage. 25:653–660.
O'Craven KM, Rosen BR, Kwong KK, Treisman A, Savoy RL. 1997. Voluntary attention modulates fMRI activity in human MT–MST. Neuron. 18:591–598.
Oldfield RC. 1971. The assessment and analysis of handedness: the Edinburgh inventory. Neuropsychologia. 9:97–113.
Oscarsson O. 1980. Functional organization of olivary projection to the cerebellar anterior lobe. In: Courville J, DeMontigny C, Lamarre Y, editors. The inferior olivary nucleus: anatomy and physiology. New York: Raven. p. 279–289.
Passingham RE, Toni I, Rushworth MFS. 2000. Specialisation within the prefrontal cortex: the ventral prefrontal cortex and associative learning. Exp Brain Res. 133:103–113.
Pearce JM, Hall GA. 1980. A model for Pavlovian learning: variations in the effectiveness of conditioned but not of unconditioned stimuli. Psychol Rev. 87:532–552.
Penny WD, Holmes AP. 2003. Random effects analysis. In: Frackowiak RS, Friston KJ, Frith CD, Dolan RJ, Price CJ, Ashburner J, Penny WD, Zeki S, editors. Human brain function. 2nd ed. London: Academic Press. p. 843–850.
Pfaff DW. 2006. Brain arousal and information theory: neural and genetic mechanisms. Cambridge (MA): Harvard University Press.
Pollatos O, Schandry R, Auer DP, Kaufmann C. 2007. Brain structures mediating cardiovascular arousal and interoceptive awareness. Brain Res. 1141:178–187.
Pollok B, Gross J, Kamp D, Schnitzler A. 2008. Evidence for anticipatory motor control within a cerebello-diencephalic-parietal network. J Cogn Neurosci. 20:828–840.
Rizzolatti G, Luppino G, Matelli M. 1998. The organization of the cortical motor system: new concepts. Electroencephalogr Clin Neurophysiol. 106:283–296.
Ro T, Rorden C, Driver J, Rafal R. 2001. Ipsilesional biases in saccades but not perception after lesions of the human inferior parietal lobule. J Cogn Neurosci. 13:920–929.
Rottschy C, Eickhoff SB, Schleicher A, Mohlberg H, Kujovic M, Zilles K, Amunts K. 2007. Ventral visual cortex in humans: cytoarchitectonic mapping of two extrastriate areas. Hum Brain Mapp. 28:1045–1059.
Rowe J, Hughes L, Eckstein D, Owen AM. 2008. Rule-selection and action-selection have a shared neuroanatomical basis in the human prefrontal and parietal cortex. Cereb Cortex. 18:2275–2285.
Sakai K, Hikosaka O, Takino R, Miyauchi S, Nielsen M, Tamada T. 2000. What and when: parallel and convergent processing in motor control. J Neurosci. 20:2691–2700.
Scheperjans F, Eickhoff SB, Hömke L, Mohlberg H, Hermann K, Amunts K, Zilles K. 2008. Probabilistic maps, morphometry, and

variability of cytoarchitectonic areas in human superior parietal cortex. Cereb Cortex. 18:2141–2157.
Scheperjans F, Hermann K, Eickhoff SB, Amunts K, Schleicher A, Zilles K. 2008. Observer-independent cytoarchitectonic mapping of the human superior parietal cortex. Cereb Cortex. 18: 846–867.
Schultz J, Lennert T. 2009. BOLD signal in intraparietal sulcus covaries with magnitude of implicitly driven attention shifts. Neuroimage. 45:1314–1328.
Schultz W, Dickinson A. 2000. Neuronal coding of prediction errors. Annu Rev Neurosci. 23:473–500.
Serences JT, Shomstein S, Leber AB, Golay X, Egeth HE, Yantis S. 2005. Coordination of voluntary and stimulus-driven attentional control in human cortex. Psychol Sci. 16:114–122.
Shapiro K, Hillstrom AP, Husain M. 2002. Control of visuotemporal attention by inferior parietal and superior temporal cortex. Curr Biol. 12:1320–1325.
Shulman GL, Astafiev SV, Franke D, Pope DLW, Snyder AZ, McAvoy MP, Corbetta M. 2009. Interaction of stimulus-driven reorienting and expectation in ventral and dorsal frontoparietal and basal ganglia-cortical networks. J Neurosci. 29:4392–4407.
Snyder LH, Batista AP, Andersen RA. 1997. Coding of intention in the posterior parietal cortex. Nature. 386:167–170.
Snyder LH, Batista AP, Andersen RA. 1998. Change in motor plan, without a change in the spatial locus of attention, modulates activity in posterior parietal cortex. J Neurophysiol. 79:2814–2819.
Strange BA, Duggins A, Penny W, Dolan RJ, Friston KJ. 2005. Information theory, novelty and hippocampal responses: unpredicted or unpredictable? Neural Netw. 18:225–230.
Thickbroom GW, Byrnesa ML, Saccoa P, Ghosha S, Morrisc IT, Mastaglia FL. 2000. The role of the supplementary motor area in externally timed movement: the influence of predictability of movement timing. Brain Res. 874:233–241.
Vandenberghe R, Gillebert CR. 2009. Parcellation of parietal cortex: convergence between lesion-symptom mapping and mapping of the intact functioning brain. Behav Brain Res. 199:171–182.
Wang L, Liu X, Guise KG, Knight RT, Ghajar J, Fan J. 2009. Effective connectivity of the fronto-parietal network during attentional control. J Cogn Neurosci. 22:543–553.
Wolpert DM, Kawato M. 1998. Multiple paired forward and inverse models for motor control. Neural Netw. 11:1317–1329.
Worsley KJ, Marrett S, Neelin P, Vandal AC, Friston KJ, Evans AC. 1996. A unified statistical approach for determining significant signals in images of cerebral activation. Hum Brain Mapp. 4:58–74.
Yamaguchi S, Zheng D, Oka T, Bokura H. 2008. The key locus of common response inhibition network for no-go and stop signals. J Cogn Neurosci. 20:1434–1442.
Yeh Y-Y, Kuo B-C, Liu H-L. 2007. The neural correlates of attention orienting in visuospatial working memory for detecting feature and conjunction changes. Brain Res. 1130:146–157.
Zeki S, Watson JD, Lueck CJ, Friston KJ, Kennard C, Frackowiak RS. 1991. A direct demonstration of functional specialization in human visual cortex. J Neurosci. 11:641–649.